Lyapunov instability of rigid diatomic molecules in three dimensions

Young-Han Shin, Dong-Chul Ihm, and Eok-Kyun Lee
Department of Chemistry, Korea Advanced Institute of Science and Technology, 373-1 Kusong-dong, Yusong-ku, Taejon, 305-701, Republic of Korea

(Received 24 February 2001; revised manuscript received 20 June 2001; published 24 September 2001)

We study the Lyapunov instability of a three-dimensional fluid composed of rigid diatomic molecules by molecular dynamics simulation. We use center-of-mass coordinates and angular variables for the configurational space variables. The spectra of Lyapunov exponents are obtained for 32 rigid diatomic molecules interacting through the Weeks-Chandler-Andersen potential for various bond lengths and densities. We show the general trends and characteristic features of the spectra of the Lyapunov exponents, and discuss the different contributions between translational and rotational degrees of freedom depending on the density and the bond length from the calculation of the projection of a certain subspace of the tangent space vectors.

DOI: 10.1103/PhysRevE.64.041106 PACS number(s): 05.20.−y, 05.45.−a, 31.15.Qg

I. INTRODUCTION

The motion of molecules in a dense fluid shows chaotic behavior and sensitive dependence on initial conditions. Their characteristic behaviors come from collisions between molecules and are described by the exponential rates of divergence or convergence of neighboring phase-space trajectories, known as the Lyapunov exponents. The sum of the first n Lyapunov exponents describes the divergence or convergence rate of an n-dimensional phase-space volume. The largest Lyapunov exponent was characterized numerically by Benettin, Galgani, and Strelcyn [1], and a general approach to the spectrum of the Lyapunov exponents was described by Shimada and Nagashima [2]. The study of the spectrum of the Lyapunov exponents through molecular dynamics simulation was pioneered by Hoover and Posch [3–7]. Since then, the Lyapunov instability has been studied for various systems, like Lorentz gas [9,10], XY models [11], hard disks or spheres [12,13], and soft disks or spheres [14–16]. Also there have been efforts to relate the spectra of the Lyapunov exponents to self-diffusion coefficients [17], and Kolmogorov-Sinai entropy h_{KS} defined as

$$h_{KS}=\sum_{\lambda_i>0}\lambda_i \tag{1}$$

to thermodynamic entropy [18,19].

Diatomic molecular fluids show a variety of features compared to atomic fluids. Due to additional rotational degrees of freedom, structural properties such as the relaxation process become much more complicated compared to that of the simple fluid. Equilibrium structures of diatomic molecular fluid, which are shown in terms of site-atom pair-correlation functions, differ strongly from monoatomic pair-correlation functions at the same thermodynamic state. On the other hand, there is a qualitative similarity in the behavior of density-dependent compressibility factors. In the previous work by Tildesley and Streett [20], it was shown that the equation of state of the hard dumbbell system can be expressed in the Carnahan-Starling form, the empirical equation of state of the hard sphere system. Also there have been various efforts to elucidate the rotational diffusion coefficients in addition to the translational diffusion coefficients from the studies of corresponding autocorrelation functions [21–27]. As molecular systems display a much greater diversity of phases than simple atomic systems, it will be of interest in studying dynamical parameters such as Lyapunov exponents to understand the dynamics associated with rotational and translational degrees of freedom for various densities and bond lengths. Recently, there has been some progress in the study of Lyapunov instability in polyatomic molecular systems [28–31,34]. Borzsák, Posch, and Baranyai [28] studied the spectrum of Lyapunov exponents in a fluid composed of rigid diatomic molecules moving in two-dimensional space, and Milanović, Posch, and Hoover [29] studied the Lyapunov instability of the two-dimensional hard dumbbell systems. Calvo calculated the largest Lyapunov exponent of nitrogen clusters [30] and methane clusters [31] to explain the melting behavior of small molecular clusters. Borzsák and Calvo used Lagrange multipliers and the quaternion coordinates method, respectively, to fix the bond length of each molecule. However, due to unavoidable computer precision errors, bond length d or constraint of the quaternions deviates from the fixed value as the numerical integration progresses. Thus it requires periodic normalization of the bond length d or the constraint of the quaternions during the iterations. Recently developed rotation-SHAKE (RSHAKE) [32], in which the entire rotation matrix is evolved using the scheme of McLachlan and Scovel [33], can be one of the promising candidates for the calculation of the spectrum of Lyapunov exponents of rigid polyatomic systems if this method is further developed so that it can be applied for the evaluation of the Lyapunov exponents using the tangent space method.

It seems to be desirable to use the polar angle representation to observe the translational and rotational motion of an individual diatomic molecule separately. Kum, Shin, and Lee [34] developed a method for calculating the spectrum of Lyapunov exponents of a fluid composed of two-dimensional rigid diatomic molecules. This method does not require periodic rescaling of the bond length that causes drift of the total energy of the system. However, application of this polar angle representation to the three-dimensional diatomic molecular fluid requires great care due to the singularity occur-

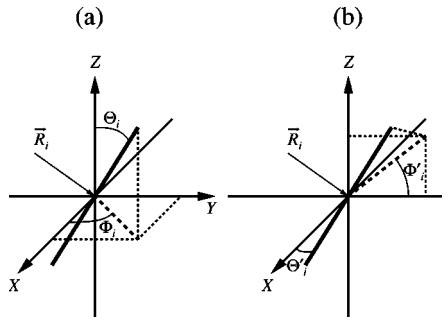

FIG. 1. Geometry of the model used to simulate homonuclear diatomic fluid. (a) *Representation A.* Θ_i is the angle from Z axis to the molecular axis and Φ_i is the angle from X axis to the projection of the molecular axis on the X-Y plane. (b) *Representation B.* Θ'_i is the angle from X axis to the molecular axis and Φ'_i is the angle from Y axis to the projection of the molecular axis on the $Y-Z$ plane.

ring in the equations of motion. We first introduce the center-of-mass coordinates vector $\{\vec{R}\}$ and two angular variables $\{\Theta,\Phi\}$ and their conjugate momenta $\{\vec{P},P_\Theta,P_\Phi\}$ for each diatomic molecule to describe the motion of the individual diatomic molecule. To avoid the singularity occurring in the equations of motion when Θ_i is near zero or π, we change the definitions of the spherical angular variables from Θ_i, Φ_i to Θ'_i, Φ'_i, or vice versa [21]. This change does not modify the expression of the center-of-mass Cartesian coordinates. Therefore the computations of the interatomic forces are independent of the angular definitions. This technique enables us to evaluate the equations of motion with sufficient accuracy. On the other hand, in the case where the tangent space method is used for the calculation of the Lyapunov exponents, the phase-space coordinates system that defines the initial tangent space vector is not allowed to change during the integration of the propagator obtained from the linearized equations of motion. This means that we cannot apply this technique for the calculation of the Lyapunov exponents. However, this problem was solved by using a sophisticated integrator.

The remainder of this paper is organized as follows. In Sec. II we briefly describe the numerical methods to evaluate the time evolution of the system composed of rigid diatomic molecules in phase space and in tangent space. In Sec. III we show the results and discussion of the thermodynamical behaviors and the Lyapunov spectra for diatomic molecular fluid. Finally, conclusions follow in Sec. IV.

II. DESCRIPTION OF THE MODEL

The bulk system that we study is composed of N rigid diatomic molecules with periodic boundary conditions. The ith molecule has a bond length d_i and mass M_i. A schematic representation of the model of diatomic molecules is given in Fig. 1. In this figure $\vec{R}_i$ denotes the configurational vector of the ith molecular center-of-mass

$$\vec{R}_i=(X_i,Y_i,Z_i)^t, \tag{2}$$

where the superscript t refers to the matrix transposition and Θ_i and Φ_i denote two angular coordinates of the ith molecular axis. The Cartesian coordinates vector $\vec{r}_{i,k}$ of the kth atom belonging to the ith molecule is

$$\vec{r}_{i,k}=\vec{R}_i-(-1)^k\frac{d_i}{2}\vec{S}_i, \tag{3}$$

where $i=1,2,\ldots,N$ and $k=1,2$. $\vec{S}_i$ is a column vector written as

$$\vec{S}_i=(\sin\Theta_i\cos\Phi_i,\ \sin\Theta_i\sin\Phi_i,\ \cos\Theta_i)^t. \tag{4}$$

Then, the bond length d_i for the ith molecule $d_i=|\vec{r}_{i,1}-\vec{r}_{i,2}|$ is naturally fixed without using any additional constraint.

In this paper, a homogeneous system ($d_i=d$ and $M_i=M$ for $i=1,\ldots,N$) is assumed, and reduced units are used, for which the Lennard-Jones parameters ϵ and σ, and the molecular mass M (atomic mass $m=M/2$) are unity [35]. Then the kinetic energy K of the three-dimensional diatomic molecular system is the sum of a translational part and a rotational part, and is written as

$$K=\sum_{i=1}^{N}\left(\frac{1}{2}M_i\vec{v}_{i,cm}^2+\frac{1}{2}I_{i,cm}\omega_i^2\right) \tag{5}$$

$$=\frac{M}{2}\sum_{i=1}^{N}\left[\dot{\vec{R}}_i^2+\left(\frac{d}{2}\right)^2[\dot{\Theta}_i^2+\sin^2(\Theta_i)\dot{\Phi}_i^2]\right], \tag{6}$$

where $\vec{v}_{i,cm}$ is the center-of-mass velocity of the ith molecule, $I_{i,cm}$ is the moment of inertia of a body of mass M about an axis through its center-of-mass, and ω_i is the angular speed of the ith molecule.

If the pairwise additive potential function $\phi(r)$ is assumed, the potential energy Φ can be written as

$$\Phi=\sum_{i<j}^{N}\sum_{\alpha,\beta=1}^{2}\phi(r_{ij}^{\alpha\beta}), \tag{7}$$

where $r_{ij}^{\alpha\beta}$ is the distance between the αth atom of the ith molecule and the βth atom of the jth molecule,

$$r_{ij}^{\alpha\beta}=|\vec{r}_{i,\alpha}-\vec{r}_{j,\beta}|. \tag{8}$$

The intermolecular potential function that is used in this paper is the Weeks-Chandler-Andersen (WCA) potential $\phi_{WCA}(r)$ with a cutoff distance $r_c=2^{1/6}$ [8],

$$\phi_{WCA}(r)=\begin{cases}\phi_{LJ}(r)+1, & r<r_c\\ 0, & r\geqslant r_c,\end{cases} \tag{9}$$

where r_c is the location of the minimum of the Lennard-Jones potential $\phi_{LJ}(r)=4[(1/r)^{12}-(1/r)^6]$.

Then the Lagrangian L of the system composed of N diatomic molecules is

$$L=K-\Phi \tag{10}$$

and the equations of motion for each molecule are

$$\dot{\vec{R}}_i = \dot{\vec{P}}_i,$$

$$\dot{\Theta}_i = P_{\Theta_i}/I,$$

$$\dot{\Phi}_i = \frac{1}{I \sin^2 \Theta_i} P_{\Phi_i},$$

$$\dot{\vec{P}}_i = -\frac{\partial V}{\partial \vec{R}_i}$$

$$\dot{P}_{\Theta_i} = \frac{\cos \Theta_i}{I \sin^3 \Theta_i} P_{\Phi_i}^2 - \frac{\partial V}{\partial \Theta_i},$$

$$\dot{P}_{\Phi_i} = -\frac{\partial V}{\partial \Phi_i}, \tag{11}$$

where I is the moment of inertia with respect to the axis perpendicular to the molecular axis that is $M(d/2)^2$. The term $\sin\Theta_i$ in Eq. (11) causes serious numerical errors in computation of $\dot{\Phi}_i$ and $\dot{P}_{\Theta_i}$ when Θ_i is nearly 0 or π. To avoid this difficulty, when $\sin\Theta_i$ is smaller than 0.1, we change the definition of the spherical angles Θ_i, Φ_i (*representation A*) to Θ_i', Φ_i' (*representation B*) or vice versa [Fig. 1] [21]. This transformation can be obtained from the following relations:

$$\sin\Theta_i \cos\Phi_i = \cos\Theta_i',$$

$$\sin\Theta_i \sin\Phi_i = \sin\Theta_i' \cos\Phi_i',$$

$$\cos\Theta_i = \sin\Theta_i' \sin\Phi_i'. \tag{12}$$

The equations of motion in the *representation B* are the same as Eq. (11) except that the prime ($'$) is inserted in the angular variables and the angular momenta. Also, since the intermolecular forces expressed by the diatomic potential model are independent of the angular definitions, the angular momenta and the torques are not modified by this change. This method keeps the relative variation for total energy below the order of 10^{-5} during 1.0×10^3 time units and the numerical precision is of the same order as the case of the two-dimensional diatomic fluid system [34], where the change of the definition of the angular variables is not necessary. The Runge-Kutta method of order four was used for the numerical integration of Eq. (11) with a time step $\Delta t^* = 0.001$. At each time step, the atomic coordinates for each molecule were obtained from the center-of-mass coordinates and the rotational angles according to the coordinates transformation equation, Eq. (3).

For the evaluation of the Lyapunov exponents, it is useful to represent the state of the system by the $10N$-dimensional state vector $\vec{\Gamma} = \{X_i, Y_i, Z_i, \Theta_i, \Phi_i, P_{X_i}, P_{Y_i}, P_{Z_i}, P_{\Theta_i}, P_{\Phi_i}\}$, where $i = 1, \ldots, N$. The equations of motion [Eq. (11)] can be conveniently written by the state vector $\vec{\Gamma}(t)$ as follows:

$$\dot{\vec{\Gamma}}(t) = \vec{G}(\vec{\Gamma}(t)), \tag{13}$$

where $\vec{G}(\vec{\Gamma}(t))$ refers to the right-hand side of Eq. (11). The solution of Eq. (13) defines the flow $\vec{\Gamma}(t) = \Phi_t(\vec{\Gamma}(0))$ in the phase space. We consider a neighbor trajectory $\vec{\Gamma}'(0)$ displaced from $\vec{\Gamma}(0)$ by $\delta\vec{\Gamma}(0)$,

$$\vec{\Gamma}'(0) = \vec{\Gamma}(0) + \delta\vec{\Gamma}(0). \tag{14}$$

From this equation we can define the tangent vector $\vec{\delta}(0)$,

$$\vec{\delta}(0) = \lim_{s\to 0} \frac{\vec{\Gamma}'(0) - \vec{\Gamma}(0)}{s}, \tag{15}$$

associated with an initial perturbation $\vec{\Gamma}'(0) - \vec{\Gamma}(0)$ from the reference trajectory in the phase space. Here s is the norm of the initial perturbation $\delta\vec{\Gamma}(0)$. As time goes on, the associated tangent vector evolves as

$$\vec{\delta}(t) = \lim_{s\to 0} \frac{\vec{\Gamma}'(t) - \vec{\Gamma}(t)}{s}. \tag{16}$$

The stability of the reference trajectory due to the initial infinitesimal perturbation is determined by the change of the magnitude of $\vec{\delta}(t)$. Consequently, $\vec{\delta}(t)$ may be viewed as a vector co-moving and co-rotating with the phase flow in the immediate neighborhood of the phase point. The equations of motion for $\vec{\delta}(t)$ are obtained by linearizing Eq. (13)

$$\dot{\vec{\delta}}(t) = M(\vec{\Gamma}(t))\vec{\delta}(t) + O(\vec{\delta}^2(t)), \tag{17}$$

where $M(\vec{\Gamma}) = \partial\vec{G}(\vec{\Gamma})/\partial\vec{\Gamma}$ is the matrix that defines the stability of the phase point $\vec{\Gamma}$. With the time ordering operator T, the formal solution of Eq. (17) can be expressed as

$$\vec{\delta}(t) = T \exp\left[\int_0^t M(t')dt'\right]\vec{\delta}(0). \tag{18}$$

Then, the largest Lyapunov exponent λ_1 is calculated from

$$\lambda_1 = \lim_{t\to\infty} \frac{1}{t} \ln\left(\frac{|\vec{\delta}_1(t)|}{|\vec{\delta}_1(0)|}\right). \tag{19}$$

The second largest Lyapunov exponent λ_2 can be obtained by adding two neighbor tangent vectors that do not lie on the same plane and calculating the area made by the tangent vectors,

$$\lambda_1 + \lambda_2 = \lim_{t\to\infty} \frac{1}{t} \ln\left(\frac{|\vec{\delta}_1(t)\times\vec{\delta}_2(t)|}{|\vec{\delta}_1(0)\times\vec{\delta}_2(0)|}\right)$$

$$= \lim_{t\to\infty} \frac{1}{t} \ln\left(\frac{|\vec{\delta}_1(t)||\vec{\delta}_2^{\perp}(t)|}{|\vec{\delta}_1(0)||\vec{\delta}_2^{\perp}(0)|}\right)$$

TABLE I. The numerical values of the largest Lyapunov exponent λ_1, the Kolmogorov-Sinai entropy h_{KS}, the smallest positive Lyapunov exponent λ_{156}, and four vanishing exponents (λ_{157}, λ_{158}, λ_{159}, λ_{160}) for various bond lengths d/σ ranging from 0.2 to 1.0 with a fixed number density $\rho^*=0.5$. All quantities are given in reduced units.

d/σ	0.2	0.3	0.4	0.5	0.6	0.7	0.8	0.9	1.0
ρ_a	0.6	0.65	0.7	0.75	0.8	0.85	0.9	0.95	1.0
λ_1	5.548	5.703	5.741	5.781	5.746	5.648	5.434	5.133	4.127
h_{KS}	15.42	16.90	17.17	16.67	15.60	14.12	12.50	10.92	9.406
λ_{156}	0.097	0.105	0.116	0.059	0.062	0.042	0.042	0.026	0.030
λ_{157}	0.027	0.016	0.021	0.015	0.018	0.011	0.007	0.009	0.009
λ_{158}	0.009	0.007	0.010	0.008	0.009	0.007	0.007	0.008	0.007
λ_{159}	0.008	0.005	0.006	0.007	0.008	0.006	0.007	0.007	0.007
λ_{160}	0.003	0.005	0.005	0.007	0.007	0.006	0.005	0.005	0.006

$$= \lambda_1 + \lim_{t\to\infty} \frac{1}{t} \ln\left(\frac{|\vec{\delta}_2^{\perp}(t)|}{|\vec{\delta}_2^{\perp}(0)|} \right)$$

$$\lambda_2 = \lim_{t\to\infty} \frac{1}{t} \ln\left(\frac{|\vec{\delta}_2^{\perp}(t)|}{|\vec{\delta}_2^{\perp}(0)|} \right), \tag{20}$$

where $|\vec{\delta}_2^{\perp}|$ is defined as $|\vec{\delta}_1 \times \vec{\delta}_2|/|\vec{\delta}_1|$. In this way, the discrete spectrum of the Lyapunov exponents $\lambda_1, \ldots, \lambda_{N_{max}}$ can be obtained successively, where N_{max} is the number of all phase-space variables. In the actual calculations, we use the classical method of Benettin *et al.* [1] refined by Hoover and Posch [3–7] that requires continuous orthonormalization to avoid the very small angles between tangent vectors and the exponential divergence of $|\vec{\delta}_1(t)|$. For this, we assume that the system is ergodic and the exponents are independent of the initial phase point $\Gamma(0)$ and the initial phase-space separations $\vec{\delta}(0)$. The Lyapunov exponents can be ordered, $\lambda_1 \geqslant \lambda_2 \geqslant \cdots \geqslant \lambda_{N_{max}}$, and the whole set is referred to as the spectrum of the Lyapunov exponents.

The integration of Eq. (17) requires a highly accurate integrator. Our method, which employs two definitions of the spherical angles depending on the orientation of individual molecules, is not applicable as the calculation of Eq. (17), since during the time averaging process described in Eq. (19) the tangent vector $\vec{\delta}_i(t)$ has to be represented by the same spherical angular variables that $\vec{\delta}_i(0)$ is represented by. This can be achieved by transforming all the molecules described in *representation B* to the *representation A* during the time averaging processes. However, a straightforward application of the Runge-Kutta method of order four for the integration of Eq. (17) cannot produce precise numerical results of Lyapunov exponents due to the singular terms appearing in the matrix $M(\vec{\Gamma}(t))$ in Eq. (17) when Θ is near 0 or π. By estimating the local truncation error depending on the time step size, the magnitude of this numerical error can be kept below a certain prescribed tolerance by automatically adjusting the time step size in the Runge-Kutta method. In the present work, we found that for the integration of Eq. (17), the adaptive Runge-Kutta-Fehlberg method of order four keeps the truncation error within a desired precision [36].

III. RESULTS AND DISCUSSION

We consider a system of 32 interacting diatomic molecules moving in a cubic periodic box. The initial arrangement of the center-of-mass coordinates of the molecules is set to an fcc structure with the molecular axes chosen to avoid high potential energy and the initial angular velocities set to zero. The initial values of center-of-mass velocities and each element of the initial tangent vectors are chosen randomly.

The initial temperature was set sufficiently high to obtain a random configuration. Then velocities were repeatedly scaled to adjust to the required temperature 0.7 within a 1% deviation. Once the required temperature was obtained, iterations over 5.0×10^2 time units were performed to reach equilibrium. After equilibrium was obtained, iterations over 1.0×10^3 time units were performed to evaluate the thermodynamic data and the Lyapunov exponents. Throughout all of the simulations, we used a microcanonical system that conserves the total energy E.

The reduced molecular number density $\rho^*=N\sigma^3/V=\rho\sigma^3$ is varied from 0.2 to 0.5 and the bond length d/σ is varied from 0.2 to 1.0 during our simulations. The bond length d describes the anisotropy of the molecular shape, so we define the anisotropy-dependent density ρ_a as

$$\rho_a = \frac{N}{V}\sigma^2(\sigma + d), \tag{21}$$

where $\sigma=1$ in the present simulation. This is, roughly speaking, the ratio of the occupied volume to the total [28].

In a system of $10N$ dimensions, the conservation of total energy (one), center-of-mass (three), total momentum (three), and the natural behavior in the flow direction (one) causes eight Lyapunov exponents to be zero. In Table I, our numerical calculations show that these values are consistently smaller than 0.02 for a whole range of densities, whereas the smallest positive exponents are still significantly larger than zero. Table I also includes the largest Lyapunov

TABLE II. Thermodynamic quantities characterizing a microcanonical system of 500 diatomic molecules for various bond lengths d/σ ranging from 0.2 to 1.0 with a fixed number density $\rho^*=0.5$. All the quantities are given in reduced units. $\langle K\rangle$ is the average kinetic energy per particle, $\langle V\rangle$ is the average potential energy per particle, E is the total energy, T is the temperature, and T_α is the temperature of α component.

d/σ	0.2	0.3	0.4	0.5	0.6	0.7	0.8	0.9	1.0
ρ_a	0.6	0.65	0.7	0.75	0.8	0.85	0.9	0.95	1.0
$\langle V\rangle$	0.286	0.383	0.510	0.665	0.870	1.116	1.404	1.722	2.048
E	2.036	2.139	2.275	2.419	2.630	2.873	3.160	3.481	3.806
k_BT	0.700	0.702	0.706	0.702	0.704	0.703	0.702	0.704	0.703
k_BT_X	0.699	0.703	0.706	0.701	0.704	0.703	0.702	0.703	0.703
k_BT_Y	0.699	0.701	0.706	0.702	0.704	0.703	0.702	0.703	0.703
k_BT_Z	0.699	0.703	0.704	0.700	0.703	0.702	0.701	0.704	0.602
k_BT_Θ	0.700	0.703	0.707	0.701	0.706	0.704	0.703	0.704	0.704
k_BT_Φ	0.702	0.703	0.707	0.703	0.705	0.704	0.704	0.704	0.705

exponent λ_1 and the Kolmogorov-Sinai entropy h_{KS} for nine bond lengths d/σ equal to 0.2, 0.3, 0.4, 0.5, 0.6, 0.7, 0.8, 0.9, and 1.0 with a fixed number density $\rho^*=0.5$. All the quantities are given in reduced units. The thermodynamic information of the corresponding systems is given in Table II. The velocities were repeatedly rescaled to keep the average kinetic energy of molecules equal to 1.75, which corresponds to 0.35 for each translational and rotational degrees of freedom. Throughout all of the simulations, as is shown in Table II, the total kinetic energy remains constant and the equipartition shows little deviation from the targeted value.

Figures 2(a)–(d) show the positive branches of the full spectra of Lyapunov exponents for various bond lengths d/σ ranging from 0.2 to 1.0. Due to the Smale pairing symmetry for symplectic systems, the negative branch is obtained by reversing the sign of the positive branch. The index l numbers the exponents. In a regime of relatively low anisotropy-dependent density, due to the large relative weight of exponents in the middle of index l, the spectrum of Lyapunov exponents shows a characteristic convex feature. As the anisotropy-dependent density increases, the shape of the spectrum changes from convex to concave [15].

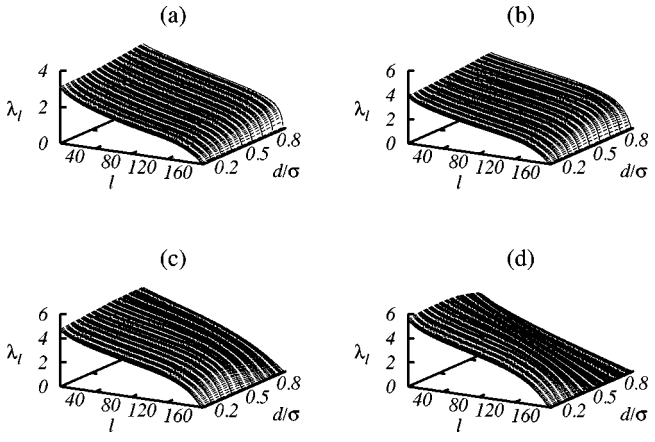

FIG. 2. Positive branch of the spectrum of Lyapunov exponents for 32 body system. ρ^* is the number density and l numbers the exponents. d is given in the units of diameter σ and λ is in units of $(\epsilon/m\sigma^2)^{1/2}$. (a) $\rho^*=0.2$, (b) $\rho^*=0.3$, (c) $\rho^*=0.4$, and (d) $\rho^*=0.5$.

In an earlier work by Tildesley and Streett [20], they calculated compressibility factors for hard dumbbell fluid, and showed that the equation of state can be well fitted to the Carnahan-Starling form with the coefficients, in this case, dependent on the elongation of the hard dumbbell. Here we examine physical meaning of the anisotropy-dependent density ρ_a from another point of view. In Fig. 3, we present the compressibility factors obtained from the calculation of thermodynamic pressure for the diatomic molecular system with $N=500$ for various ρ_a. The solid line represents the modified Carnahan-Starling equation [37] for a simple fluid interacting through the WCA potential, which is written as

$$z=\frac{P}{\rho k_BT}=\frac{1+a\,\eta+b\,\eta^2+c\,\eta^3+d\,\eta^4+e\,\eta^5+f\,\eta^6}{1-3\,\eta+3\,\eta^2+g\,\eta^3}, \tag{22}$$

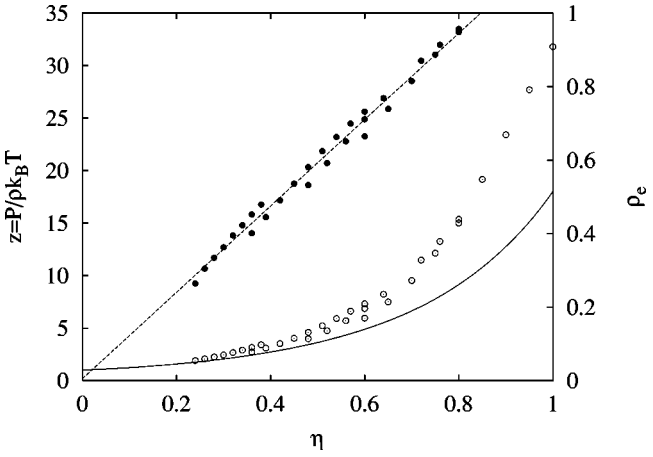

FIG. 3. Open circles are the compressibility factors of the diatomic molecular fluid with respect to the anisotropy-dependent density and the solid line represents the Carnahan-Starling equation modified by Hall for a simple fluid with the WCA potential. The relationship between the effective density and the anisotropy-dependent density is shown by solid circles. The dashed line is the linear least squares fitting between these two quantities ($\rho_e=1.17\rho_a$).

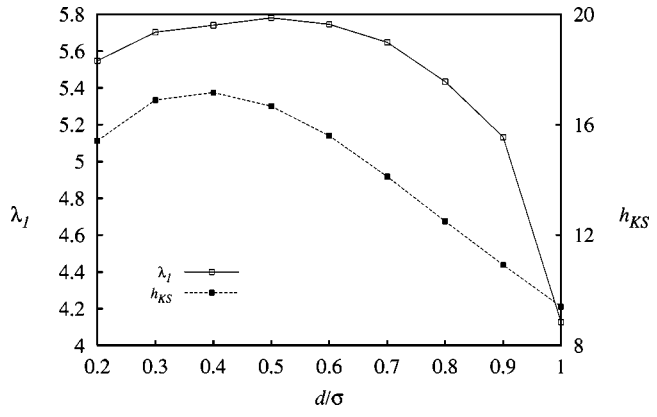

FIG. 4. The largest Lyapunov exponent λ_1 and the Kolmogorov-Sinai entropy h_{KS} as a function of d/σ for $\rho^*=0.5$. λ and h_{KS} are in units of $(\epsilon/m\sigma^2)^{1/2}$.

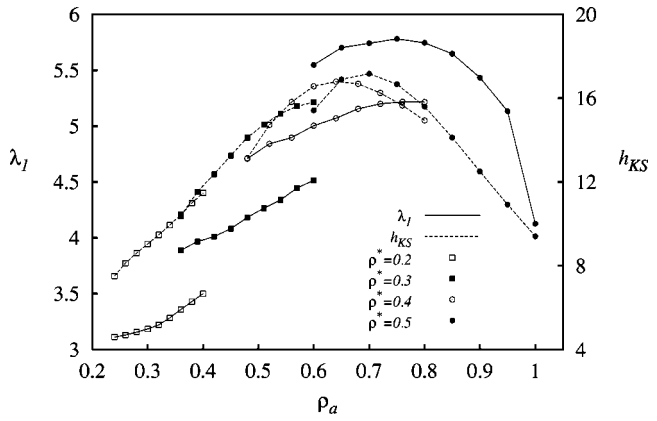

FIG. 5. The largest Lyapunov exponent and the Kolmogorov-Sinai entropy as a function of ρ_a.

where $a=-1.047$, $b=1.018$, $c=-3.011$, $d=1.017$, $e=1.754$, $f=0.01511$, $g=-0.9586$, and η is the reduced number density $\rho\sigma^3$. The open circles represent the compressibility factors for diatomic molecular fluid, and in this case, η becomes the anisotropy-dependent density ρ_a $[=\rho\sigma^2(\sigma+d)]$. The characteristic behavior of $P/\rho k_B T$ of the diatomic molecular system has similar patterns to that of soft sphere system with WCA potential. Furthermore by defining effective density ρ_e as 1.17ρ, we found that the equation of state for the diatomic molecular system as a function of ρ_e can be well fitted to the empirical equation of the state of simple fluid with the WCA potential. In the literature on hard dumbbells [20], two different conventions have been used to express density in reduced units $\rho\chi^3$, where ρ is the number density and χ is a characteristic length. The first of these takes, as the characteristic length, the atomic diameter σ and the second takes the diameter of a sphere having a volume equal to that of the hard dumbbell. On the other hand, according to our study the effective density defined from the comparison of the equation of state between simple fluid and diatomic molecular fluid is consistently larger than the anisotropy-dependent density. This means that the effective volume of a diatomic molecule is larger than the volume defined by σ of the WCA potential and the bond length d.

Next, the largest Lyapunov exponent and the Kolmogorov-Sinai entropy h_{KS} are shown as a function of d for $\rho^*=0.5$ in Fig. 4. This figure shows a single maximum that is possibly related the transition from fluid state to solid state as the anisotropy-dependent density increases. The largest Lyapunov exponent λ_1 decreases above $d/\sigma=0.5$ and the maximum of the Kolmogorov-Sinai entropy h_{KS} occurs at about $d/\sigma=0.4$. Recall that, in the case of simple fluid, each of h_{KS} and λ_1 has a single maximum as a function of the density and the maximum of h_{KS} is shifted toward lower density with respect to the location of the maximum for λ_1. Such behaviors of λ_1 and h_{KS} for simple fluid systems are also reflected in the diatomic molecular system by identifying the anisotropy-dependent density of diatomic molecular fluid with the number density of simple fluid (see Fig. 5). One of the important future works will be to verify whether the minor irregularity in the detailed structure can disappear in the thermodynamic limit or not.

It is instructive to examine the dynamics of the tangent vectors in the subspaces associated with special degrees of freedom between two systems have the equal anisotropy-dependent density but different bond lengths and number densities. If we describe the phase space as the product of the center-of-mass configuration space Q, the respective momentum space P_Q, the angular orientation space Ω, and the associated angular momentum space P_Ω, the tangent space is also decomposed into respective subspaces TQ, TP_Q, $T\Omega$, and TP_Ω [28]. Then the mean-squared value of the projection of tangent vector $\vec{\delta}_l$ onto TX subspace can be defined as

$$\langle \vec{\delta}^2_{X,l}\rangle = \langle \mathcal{P}(X)\,\vec{\delta}_l \cdot \mathcal{P}(X)\,\vec{\delta}_l\rangle, \tag{23}$$

where X is one of Q, P_Q, Ω, and P_Ω, and $\mathcal{P}(X)$ is the projection operator to the TX subspace. The diagonal matrix with the element $\mathcal{P}_{\alpha\alpha}(X)$ is equal to unity, if the α axis of $\vec{\delta}_l$ belongs to X, and equal to zero, otherwise. Figure 6 shows the mean-squared values of the projection of tangent vectors to TX subspace $\langle \vec{\delta}^2_{X,l}\rangle$ ($X=Q$, P_Q, Ω or P_Ω) for two different cases where they have the same anisotropy-dependent density but have different number density and bond lengths. l is the index of the total 320 tangent space vectors that span the tangent space. Notice that, even though an individual component is not symmetric, the overall patterns are symmetric with respect to the center. Due to the Hamiltonian nature of the system, an increase of instability accumulated in one subspace is always accompanied with a decrease of instability in its conjugate subspace. Eight of the Lyapunov exponents vanishes for the reasons given above, so the corresponding $\vec{\delta}^2_{X,l}$ has no meaning, since Gram-Schmidt orthogonalization has no ordering effect on the directions of their tangent vectors.

When the system has low anisotropy-dependent density, only a small portion of the mean-squared length of $\vec{\delta}_1$ is contributed from the momentum space. However this value rises rapidly as ρ_a increases. This means that the instability of the phase-space trajectory is accumulated in the momentum space in high density regions. Furthermore, the contribution from the angular momentum space increases more

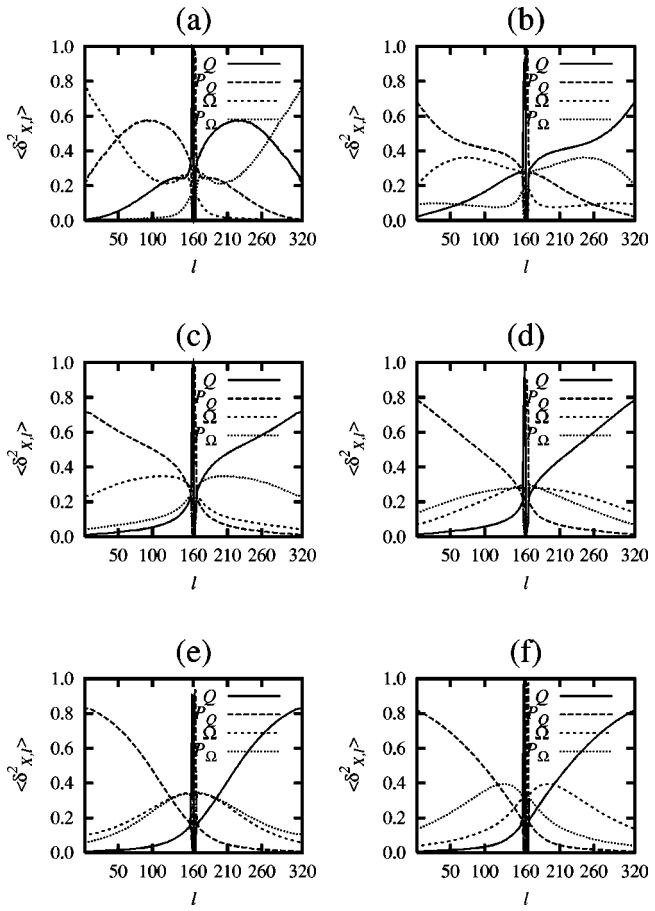

FIG. 6. Mean-squared values of the projection of tangent vectors $\vec{\delta}_l$ to the TX subspace. (a) $\rho_a=0.36$ ($d=0.2$,$\rho^*=0.3$), (b) $\rho_a=0.36$ ($d=0.8$,$\rho^*=0.2$), (c) $\rho_a=0.60$ ($d=0.5$,$\rho^*=0.4$), (d) $\rho_a=0.60$ ($d=1.0$,$\rho^*=0.3$), (e) $\rho_a=0.80$ ($d=0.6$,$\rho^*=0.5$), and (f) $\rho_a=0.80$ ($d=1.0$,$\rho^*=0.4$).

rapidly than the contribution from the translational momentum space. Figure 6 shows this trend clearly.

The two states that have the same anisotropy-dependent density present different dynamics at molecular level depending on the bond lengths and the number densities. In Fig. 6, the contributions of the tangent vectors to TX subspace $\langle \vec{\delta}^2_{X,l} \rangle$ ($X=Q$, P_Q, Ω or P_Ω) are compared with two systems having the same anisotropy-dependent density but having the different bond length and the number density. For the systems with relatively low ρ_a, the contribution of $\langle \vec{\delta}^2_{\Omega,l} \rangle$ to the instability of the phase-space trajectory is larger than that of $\langle \vec{\delta}_{P_\Omega,l} \rangle$ in relatively low ρ_a and the difference between these two contributions is larger for the systems with small d as can be seen from the comparisons between Figs. 6(a) and 6(b). As ρ_a increases, this difference decreases as can be seen in Figs. 6(c) and 6(d), and for the case of $\rho_a=0.8$, the contribution of $\langle \delta^2_{P_\Omega} \rangle$ larger than that of $\langle \delta^2_\Omega \rangle$ in the system with $d=1.0$ [compare Figs. 6(e) and 6(f)]. It is a common feature for diatomic molecular fluid and simple fluid that $P/\rho k_B T$ and the instability accumulated in the momentum space ($\langle \vec{\delta}^2_{P_Q,1} \rangle + \langle \vec{\delta}^2_{P_\Omega,1} \rangle$) increases as ρ_a increases.

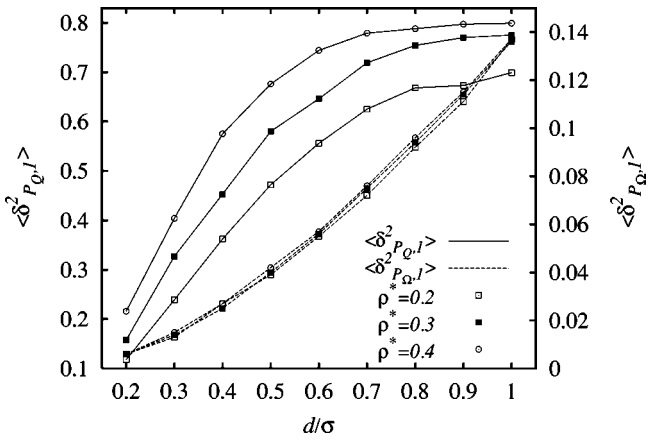

FIG. 7. Mean-squared values of the projection of a tangent vector $\vec{\delta}_1$ to the TP_Q and TP_Ω subspaces as functions of d/σ for various number densities.

However we have to note that the values of $P/\rho k_B T$ are slightly different than each other for a pair of systems that have the same ρ_a. These discrepancies seem to be partly due to the difference between the number of molecules used in the calculation of thermodynamic pressure and that used in the calculation of Lyapunov exponents. Figure 7 shows the behaviors of the squared length of $\vec{\delta}_1$ contributed from translational momentum space and angular momentum space as a function of the bond length for various number densities. The contribution from the translational momentum space is sensitive to the number density and seems to be saturated reaching a certain maximum value as the anisotropy-dependent density increases. On the other hand, the contribution from the angular momentum space shows roughly linear behavior with bond length and is insensitive to the number density.

IV. CONCLUSIONS

In this paper, we studied the instability properties of phase-space trajectories for a three-dimensional fluid composed of rigid diatomic molecules. Detailed numerical studies of the spectra of Lyapunov exponents, the Kolmogorov-Sinai entropy, and the associated tangent space vectors as a function of anisotropy-dependent density indicate that the major contributions to the instability of the phase-space trajectory come from the translational degrees of freedom and, in particular, from the translational momentum variables. This is in contrast to the case of two-dimensional diatomic molecular fluid, in which the major contribution to instability comes from the angular-momentum variables [15]. Figure 6 shows that, in general, the major contribution to the positive Lyapunov exponents, which comes from the translational center-of-mass configuration space and the angular orientation space, reduces considerably as the anisotropy-dependent density increases but these contributions change quantitatively as bond length becomes different even at the same anisotropy-dependent density [Fig. 6(f)].

Figure 7 shows that the contribution of instability from the translational momentum space is sensitive to both the

number density and the bond length of the molecules, whereas the contribution of instability from the angular momentum space seems to be dependent on only the bond length of the molecules.

The maximum of the largest Lyapunov exponent λ_1 occurs around $\rho_a = 0.75$, whereas the location of the maximum of the Kolmogorov-Sinai entropy h_{KS} is near $\rho_a = 0.7$. Although, for practical reasons, the systems contain only 32 particles, the influence of the fluid-solid phase transition on the Lyapunov instability and the Kolmogorov-Sinai entropy can be clearly seen. From the comparison of the thermodynamic pressure and the Kolmogorov-Sinai entropy of diatomic molecular fluid with those of simple fluid, we found that the anisotropy-dependent density plays a crucial role to obtain the effective density, and they are linearly proportional to each other. Our numerical method, which uses two coordinates representations to avoid the singularity occurring in the equations of motion combined with the adaptive Runge-Kutta-Fehlberg method of order four, proves that it gives sufficiently accurate numerical results for the Lyapunov instability study of the three-dimensional rigid diatomic molecular system.

ACKNOWLEDGMENTS

This work was supported by Korea Science and Engineering Foundation (Contract No. 1999-2-12100-005-3) and, in part, by grants from the Ministry of Education in Korea through Brain Korea 21.

[1] G. Benettin, L. Galgani, and J.-M. Strelcyn, Phys. Rev. A **14**, 2338 (1976).
[2] I. Shimada and T. Nagashima, Prog. Theor. Phys. **61**, 1605 (1979).
[3] W.G. Hoover and H.A. Posch, Phys. Lett. A **113**, 82 (1985).
[4] W.G. Hoover and H.A. Posch, Phys. Lett. A **123**, 227 (1987).
[5] W.G. Hoover, H.A. Posch, and S. Bestiale, J. Chem. Phys. **87**, 6665 (1987).
[6] H.A. Posch and W.G. Hoover, Phys. Rev. A **38**, 473 (1988).
[7] H.A. Posch and W.G. Hoover, Phys. Rev. A **39**, 2175 (1989).
[8] J.D. Weeks, D. Chandler, and H.C. Andersen, J. Chem. Phys. **54**, 5237 (1971).
[9] Ch. Dellago, L. Glatz, and H.A. Posch, Phys. Rev. E **52**, 4817 (1995).
[10] H. van Beijeren, J.R. Dorfman, E.G.D. Cohen, H.A. Posch, and Ch. Dellago, Phys. Rev. Lett. **77**, 1974 (1996).
[11] Ch. Dellago and H.A. Posch, Physica A **237**, 95 (1997).
[12] Ch. Dellago, H.A. Posch, and W.G. Hoover, Phys. Rev. E **53**, 1485 (1996).
[13] Ch. Dellago and H.A. Posch, Physica A **240**, 68 (1997).
[14] Ch. Dellago and H.A. Posch, Physica A **230**, 364 (1996).
[15] I. Borzsák, A. Baranyai, and H.A. Posch, Physica A **229**, 93 (1996).
[16] K.H. Kwon and B.Y. Park, J. Chem. Phys. **107**, 5171 (1997).
[17] P. Gaspard and G. Nicolis, Phys. Rev. Lett. **65**, 1693 (1990).
[18] M. Dzugutov, Nature (London) **381**, 137 (1996).
[19] M. Dzugutov, E. Aurell, and A. Vulpiani, Phys. Rev. Lett. **81**, 1762 (1998).
[20] D.J. Tildesley and W.B. Streett, Mol. Phys. **41**, 85 (1980).
[21] J. Barojas, D. Levesque, and B. Quentrec, Phys. Rev. A **7**, 1092 (1973).
[22] C. Tresser, B. Quentrec, and C. Brot, J. Phys. (France) **38**, 267 (1977).
[23] C. Brot, B. Quentrec, and C. Tresser, Mol. Phys. **34**, 1295 (1977).
[24] W.B. Streett and D.J. Tildesley, Proc. R. Soc. London, Ser. A **355**, 239 (1977).
[25] D.M. Heyes, M.J. Nuevo, and J.J. Morales, J. Chem. Soc., Faraday Trans. **94**, 1625 (1998).
[26] D.M. Heyes, M.J. Nuevo, and J.J. Morales, Mol. Phys. **93**, 985 (1998).
[27] M.H.J. Hagen, D. Frenkel, and C.P. Lowe, Physica A **272**, 376 (1999).
[28] I. Borzsák, H.A. Posch, and A. Baranyai, Phys. Rev. E **53**, 3694 (1996).
[29] Lj. Milanović, H.A. Posch, and Wm.G. Hoover, Chaos **8**, 455 (1998).
[30] F. Calvo, Phys. Rev. E **58**, 5643 (1998).
[31] F. Calvo, Phys. Rev. E **60**, 2771 (1999).
[32] A. Kol, B.B. Laird, and B.J. Leimkuhler, J. Chem. Phys. **107**, 2580 (1997).
[33] R.I. McLachlan and C. Scovel, J. Nonlinear Sci. **16**, 233 (1995).
[34] O. Kum, Y.H. Shin, and E.K. Lee, Phys. Rev. E **58**, 7243 (1998).
[35] M.P. Allen and D.J. Tildesley, *Computer Simulation of Liquids* (Oxford University Press, New York, 1987).
[36] R.L. Burden and J.D. Faires, *Numerical Analysis* (PWS, Boston, 1996).
[37] K.R. Hall, J. Chem. Phys. **57**, 2252 (1970).